Memoirs of the Faculty of Engineering and Design
Kyoto Institute of Technology 51 (March, 2003)

Accurate Computation of Forward/Inverse Continuous Wavelet Transform

Arata MASUDA

(Received September 20, 2002 ; Accepted November 1, 2002)

Abstract

This brief note describes some problems we would face in calculating continuous wavelet transform (CWT) and its inverse (ICWT), and how we can overcome those difficulties. Especially, the reconstruction error due to the parameter truncation is discussed, and a calculation method using two special functions named scaling function and residual wavelet is proposed. Also, other issues that may affect the accuracy of the calculation are briefly discussed with some tips, which might be able to help ones who try to implement the CWT/ICWT very accurately. The overall effect of those techniques results in sufficiently small reconstruction error less than one percent.

Key Words: *continuous wavelet transform; wavelet; scaling function*

1. Introduction

Wavelet transform is a mathematical tool that analyzes signals in terms of time and scale. For a one-dimensional signal made of multiple components, the wavelet transform may display those components separated in a space parametrized by time and scale. Because the "scale" basically represents the local period, or the reciprocal of the instantaneous frequency of transient signals, the wavelet transform is often used as a time-varying spectrum that can capture the temporal change of their frequency contents. Furthermore, thanks to its attractive performance in feature extraction, the wavelet transform has become one of the most standard and fundamental signal processing tools in various fields of engineering and science, including vibration/motion analysis, image processing, data compression, pattern recognition, etc.

Among a variety of categories in the world of wavelet transform, the continuous wavelet transform (CWT) may be the most fundamental one, which was first developed by Morlet to solve the oil prospecting problems in early 1980's. The standard CWT is defined as

$$(W_\phi x)(a,\ b) = \int_{-\infty}^{\infty} a^{-1/2}\overline{\phi\left(\frac{t-b}{a}\right)}x(t)dt \tag{1}$$

where $a \neq 0$ and b are the scale and shift parameters respectively, x is the signal, and ϕ is the analyzing wavelet which satisfies the following admissibility condition:

$$C := \int_{-\infty}^{\infty} \frac{|\hat{\phi}(\xi)|^2}{|\xi|}d\xi < \infty \tag{2}$$

where $\hat{\phi}$ denotes the Fourier transform of ϕ. The factor $a^{-1/2}$ is necessary to conserve the L^2-norm of the wavelets. Since there are possible variations in normalizing the wavelets, one can generalize the definition of CWT, instead of eq. (1), as[1]

$$(W_\phi^p x)(a,\ b) = \int_{-\infty}^{\infty} |a|^{-p}\overline{\phi\left(\frac{t-b}{a}\right)}x(t)dt\,. \tag{3}$$

The wavelet transform is also written in the form of a linear filter. Let $\phi_a^p(t) := |a|^{-p}\phi(t/a)$, then, the integral in eq. (3) can be rewritten as a convolution integral:

$$(W_\phi^p x)(a,\ b) = \int_{-\infty}^{\infty} \overline{\phi_a^p(t-b)}x(t)dt = \left(\overline{\phi_a^{p-}} * x\right)(b) \tag{4}$$

where $\{\cdot\}^-$ denotes the reverse with respect to time.

It is evident that the CWT is a highly redundant expression of the signal because it maps the one-dimensional signal to a two-dimensional time-scale plane. Thus, its inversion formula is not uniquely determined. The optimal one in the sense of the pseudo-inverse is given by[1]

$$x(t) = \frac{1}{C}\int_{-\infty}^{\infty}\int_{-\infty}^{\infty} \phi_a^p(t-b)\,(W_\phi^p x)(a,\ b)a^{2p-3}dbda \tag{5}$$

which, after this, is referred to by inverse CWT (ICWT).

In some cases, it is not necessary to evaluate the negative scales. This situation includes the case the analyzing wavelet is real-valued and satisfies the modified admissibility condition:

$$C^+ := \int_0^{\infty} \frac{|\hat{\phi}(\xi)|^2}{\xi}d\xi < \infty. \tag{6}$$

In this case, the ICWT will be[1]

$$x(t) = \frac{1}{C^+}\int_0^{\infty}\int_{-\infty}^{\infty} \phi_a^p(t-b)\,(W_\phi^p x)(a,\ b)a^{2p-3}dbda\,. \tag{7}$$

After this, we deal with admissible real-valued wavelets to simplify the problem.

Numbers of research groups have reported various work on the numerical implementation of CWT/ICWT. Most of them focussed on fast and efficient computation of CWT/ICWT, and some of which have developed sophisticated algorithms based on the multiresolution analysis[2].

Nevertheless, one may experience significant errors in calculating CWT/ICWT. The most important reason of those errors are the parameter truncation. The integrals in eqs. (3) and (7) should be performed on the infinite intervals, however, in practice, one has to truncate the intervals at certain boundaries. As a result, significant amount of information would be lost in the calculation. Especially, the scale integral in the reconstruction formula (7) is critical.

In this paper, a complete solution to this problem is presented, a part of which has been

reported in the author's previous paper[3]. Two representative functions, called the scaling function and the residual wavelet, are introduced to compensate the lost information. Then, those functions for two classes of wavelets will be developed. Also, other problems that may affect the accuracy of the calculation are briefly discussed. Finally, a simple calculation is performed to see how accurate the CWT/ICWT are computed using the proposed techniques.

2. Problems Related to Parameter Truncation

In the ICWT given by eq. (7), it is necessary to evaluate the integral from 0 to ∞ with respect to the scale a, and the integral from $-\infty$ to ∞ with respect to the shift b. Because it is impossible to calculate the infinite integral in a numerical way, the influence of the parameter truncation should be considered carefully.

2.1 Errors due to scale truncation and relief

First, for the scale parameter, let us suppose to take only $a \in [a_{\min}, a_{\max}]$ in the reconstruction. Then, the reconstructed signal would be significantly distorted due to the scale truncation, especially if the original signal has a DC component and/or high frequency components. To handle the truncation-induced errors, we divide the scale integral in the right hand side of eq. (7) into three parts:

$$x(t) = x_0(t) + x_1(t) + x_2(t), \tag{8}$$

$$x_0(t) = \frac{1}{C^+} \int_0^{a_{\min}} \int_{-\infty}^{\infty} \phi_a^p(t-b_0)\,(W_\phi^p x)\,(a,\ b_0)\,a^{2p-3}\,db_0\,da\,, \tag{9}$$

$$x_1(t) = \frac{1}{C^+} \int_{a_{\min}}^{a_{\max}} \int_{-\infty}^{\infty} \phi_a^p(t-b_1)\,(W_\phi^p x)\,(a,\ b_1)\,a^{2p-3}\,db_1\,da\,, \tag{10}$$

$$x_2(t) = \frac{1}{C^+} \int_{a_{\max}}^{\infty} \int_{-\infty}^{\infty} \phi_a^p(t-b_2)\,(W_\phi^p x)\,(a,\ b_2)\,a^{2p-3}\,db_2\,da \tag{11}$$

where $x_1(t)$ is the reconstructed signal evaluated with truncated scales, while $x_0(t)$ and $x_2(t)$ are the components having the scales below/above the boundaries that can lead to significant reconstruction errors.

However, the error will be compensated if we can evaluate these components and involve them in the reconstruction. Mallat[4] showed that, for $p = 1/2$, introducing a function, so-called "scaling function", one can evaluate the low frequency component $x_2(t)$. This idea can be applied to the general case with arbitrary p as described as follows.

The scaling function ϕ is defined as a function which satisfies the following equation:[4]

$$\left|\hat{\phi}(\omega)\right|^2 := \int_1^{\infty} \left|\hat{\phi}(a\omega)\right|^2 \frac{da}{a}\,. \tag{12}$$

First, we rewrite eq. (11) using a convolution integral as

$$x_2(t) = \frac{1}{C^+} \int_{a_{\max}}^{\infty} \{\phi_a^p * (W_\phi^p x)\,(a, \cdot)\}\,(t)\,a^{2p-3}\,da \tag{13}$$

where " • " indicates the variable over which the convolution is taken. Furthermore, substituting the filter expression of CWT given by eq. (4) into eq. (13) yields

$$x_2(t) = \frac{1}{C^+}\int_{a_{\max}}^{\infty}\left(\phi_a^p * \overline{\phi_a^{p-}} * x\right)(t)a^{2p-3}da\,. \tag{14}$$

Then, taking Fourier transform of both sides of eq. (14), we have

$$\hat{x}_2(\omega) = \frac{1}{C^+}\int_{a_{\max}}^{\infty}\left|\widehat{\phi_a^p}(\omega)\right|^2\hat{x}(\omega)a^{2p-3}da\,. \tag{15}$$

Considering that $\widehat{\phi_a^p}(\omega) = a^{1-p}\hat{\phi}(a\omega)$, and using the definition of the scaling function given by eq. (12), we have

$$\begin{aligned}\hat{x}_2(\omega) &= \frac{1}{C^+}\int_{a_{\max}}^{\infty}\left|\hat{\phi}(a\omega)\right|^2\hat{x}(\omega)\frac{da}{a} \\ &= \frac{1}{C^+}\int_{1}^{\infty}\left|\hat{\phi}(a_{\max}a\omega)\right|^2\hat{x}(\omega)\frac{da}{a} \\ &= \frac{1}{C^+}\left|\hat{\phi}(a_{\max}\omega)\right|^2\hat{x}(\omega).\end{aligned} \tag{16}$$

Thus, if we define that $\phi_a^p(t) := a^{-p}\phi(t/a)$, and define that

$$(W_\phi^p x)(a,\ b) := \int_{-\infty}^{\infty}\phi_a^p(t-b)x(t)dt\,, \tag{17}$$

then, the inverse Fourier transform of eq. (16) is evaluated as

$$x_2(t) = \frac{a_{\max}^{2p-2}}{C^+}\int_{-\infty}^{\infty}\phi_{a_{\max}}^p(t-b_2)\,(W_\phi^p x)(a_{\max},\ b_2)ab_2\,. \tag{18}$$

Following the same idea, we introduce a function ϕ^r, named "residual wavelet", to compensate the high frequency component $x_0(t)$. The residual wavelet is defined as a function which satisfies

$$\left|\hat{\phi}^r(\omega)\right|^2 = \int_0^1\left|\hat{\phi}(a\omega)\right|^2\frac{da}{a}\,. \tag{19}$$

In the same way as the scaling function, the following formulae are derived:

$$x_0(t) = \frac{a_{\min}^{2p-2}}{C^+}\int_{-\infty}^{\infty}\phi_{a_{\min}}^{rp}(t-b_0)\,(W_r^p x)(a_{\min},\ b_0)db_0 \tag{20}$$

where $\phi_a^{rp}(t) := a^{-p}\phi^r(t/a)$ and

$$(W_r^p x)(a,\ b) := \int_{-\infty}^{\infty}\phi_a^{rp}(t-b)x(t)dt\,. \tag{21}$$

Therefore, using eqs. (18) and (20), one can salvage the lost information outside the scale region of interest, and completely reconstruct the original signal.

It would be worth noting that both the scaling function and the residual wavelet are not uniquely determined for the given analyzing wavelet, because eqs. (12) and (19) determine only the absolute value of the Fourier transform of those functions. Thus, one can arbitrarily choose the complex phase of $\hat{\phi}(\omega)$ and $\hat{\phi}^r(\omega)$.

2.2 Shift truncation

For the shift parameters in eqs. (10), (18) and (20), if the signal is bounded in $[t_0,\ t_1]$, it is sufficient to consider them in the following range

$$\begin{aligned} &t_0 - a\tau_1^{\phi} \le b_1 \le t_1 - a\tau_0^{\phi}, \\ &t_0 - a_{\max}\tau_1^{\phi} \le b_2 \le t_1 - a_{\max}\tau_0^{\phi}, \\ &t_0 - a_{\min}\tau_1^{r} \le b_0 \le t_1 - a_{\min}\tau_0^{r} \end{aligned} \tag{22}$$

where the analyzing wavelet, the scaling function and the residual wavelet are supposed to have the compact supports on $[\tau_0^{\psi}, \tau_1^{\psi}]$, $[\tau_0^{\phi}, \tau_1^{\phi}]$, $[\tau_0^{r}, \tau_1^{r}]$, respectively. If those functions are not compactly supported, the following effective support, i.e., the minimum interval $[\tau_0, \tau_1]$ so that

$$|\psi(t)| < \varepsilon \ll 1, \; t \notin [\tau_0, \tau_1] \tag{23}$$

may be used instead.

2.3 Derivation of scaling functions and residual wavelets

2.3.1 Derivative-of-Gaussian (DOG) wavelets

Derivative-of-Gaussian (DOG) wavelets[5] are the wavelets derived from Gaussian function as

$$\psi_M(t) := (-1)^M \frac{d^M}{dt^M} e^{-t^2/2}. \tag{24}$$

The Mth-order DOG wavelet $\psi_M(t)$ has M vanishing moments, i.e.,

$$\int_{-\infty}^{\infty} \psi_M(t) t^k dt = 0, \; (k = 0, 1, \cdots\cdots, M-1), \tag{25}$$

and satisfies the following equations:

$$\frac{d^n}{dt^n}\psi_M(t) = (-1)^n \psi_{M+n}(t), \tag{26}$$

$$\underbrace{\int\int \cdots \int}_{n} \psi_M(t) dt^n = (-1)^n \psi_{M-n}(t). \tag{27}$$

The Mth-order DOG wavelet acts as a multiscale differential operator that provides a smoothed version of the Mth derivative of the signal[4].

For this class of wavelets, the scaling function and the residual wavelet are derived as follows. Let $\Psi(a, \omega)$ the primitive function of $\left|\hat{\psi}(a\omega)\right|^2 / a$, i.e.,

$$\Psi(a, \omega) := \int \left|\hat{\psi}(a\omega)\right|^2 \frac{da}{a}. \tag{28}$$

Then, the left hand sides of eqs. (12) and (19) can be evaluated as

$$\left|\hat{\phi}(\omega)\right|^2 = \Psi(\infty, \omega) - \Psi(1, \omega), \tag{29}$$

$$\left|\hat{\phi}^r(\omega)\right|^2 = \Psi(1, \omega) - \Psi(0, \omega) \tag{30}$$

Taking Fourier transform of the DOG wavelet, and substituting it into eq. (28), we have

$$\Psi(a, \omega) = 2\pi\omega^{2M} \int a^{2M-1} e^{-\omega^2 a^2} da, \tag{31}$$

then,

$$\frac{d}{da}\Psi(a, \omega) = 2\pi\omega^{2M} a^{2M-1} e^{-\omega^2 a^2}. \tag{32}$$

Assuming that $\Psi(a, \omega) = F(a, \omega) e^{-\omega^2 a^2}$, and substituting it into eq. (32), we have the

solution of eq. (32) as

$$\Psi(a,\ \omega) = -\pi \sum_{n=0}^{M-1} \frac{(M-1)!}{n!} \omega^{2n} a^{2n} e^{-\omega^2 a^2}. \tag{33}$$

Thus, we finally get

$$\hat{\phi}(\omega) = \sqrt{\pi(M-1)! \sum_{n=0}^{M-1} \frac{\omega^{2n}}{n!} e^{-\omega^2}} \tag{34}$$

$$\hat{\phi}^r(\omega) = \sqrt{\pi(M-1)! \left\{1 - \sum_{n=0}^{M-1} \frac{\omega^{2n}}{n!} e^{-\omega^2}\right\}}, \tag{35}$$

where the phase of the Fourier transform of each function is chosen as zero.

The shapes of the analyzing wavelet, the scaling function and the residual wavelet for $M = 2$ (Mexican hat) and $M = 4$ are shown in Fig. 1 and Fig. 2 with their spectra.

2.3.2 Velocity response (VR) wavelets

In the author's previous paper[3], we used a special wavelet called the velocity response (VR) wavelet to synthesize spectrum-compatible simulated earthquakes. The VR wavelet is the reverse of the velocity impulse response of a single-degree-of-freedom (SDOF) system with the natural period of 1 and the damping ratio of ζ, defined as

$$\phi(t) = \begin{cases} 0, & (t > 0) \\ -e^{2\pi\zeta t}\left(\cos 2\pi\sqrt{1-\zeta^2}\, t + \dfrac{\zeta}{\sqrt{1-\zeta^2}} \sin 2\pi\sqrt{1-\zeta^2}\, t\right), & (t \leq 0) \end{cases} \tag{36}$$

Note that the wavelet transform using the VR wavelets is causal.

For this class of wavelets, squared Fourier transform of the scaling function and the residual wavelet are derived as:

$$\left|\hat{\phi}(\omega)\right|^2 = \frac{1}{16\pi^2\zeta\sqrt{1-\zeta^2}} \left\{\frac{\pi}{2} - \tan^{-1} \frac{\omega^2 + 4\pi^2(2\zeta^2-1)}{8\pi^2\zeta\sqrt{1-\zeta^2}}\right\}. \tag{37}$$

$$\left|\hat{\phi}^r(\omega)\right|^2 = \frac{1}{16\pi^2\zeta\sqrt{1-\zeta^2}} \left\{\tan^{-1} \frac{\omega^2 + 4\pi^2(2\zeta^2-1)}{8\pi^2\zeta\sqrt{1-\zeta^2}} - \tan^{-1} \frac{2\zeta^2-1}{2\zeta\sqrt{1-\zeta^2}}\right\}, \tag{38}$$

To preserve the causality, the Fourier transform of the scaling function and the residual wavelet are derived using the factorization technique[6].

The shapes of the analyzing wavelet, the scaling function and the residual wavelet for $\zeta = 0.05$ are shown in Fig. 3 with their spectra.

3. Other Problems and Tips

3.1 Discretization of scale/shift parameters

The scale parameter is usually sampled logarithmically, while the shift parameter is sampled with sampling intervals proportional to the scales, i.e.,

$$a_j = a_{\min}\sigma^j,\ j = 0,\ 1,\ \cdots\cdots,\ J-1, \tag{39}$$

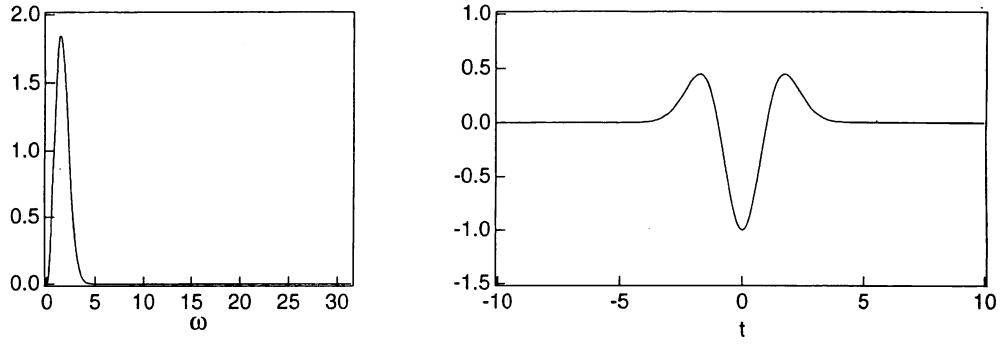

(a) Analyzing wavelet.

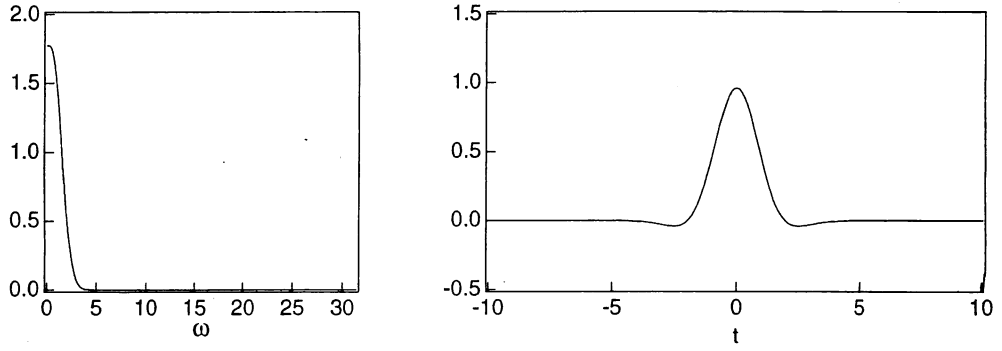

(b) Scaling function.

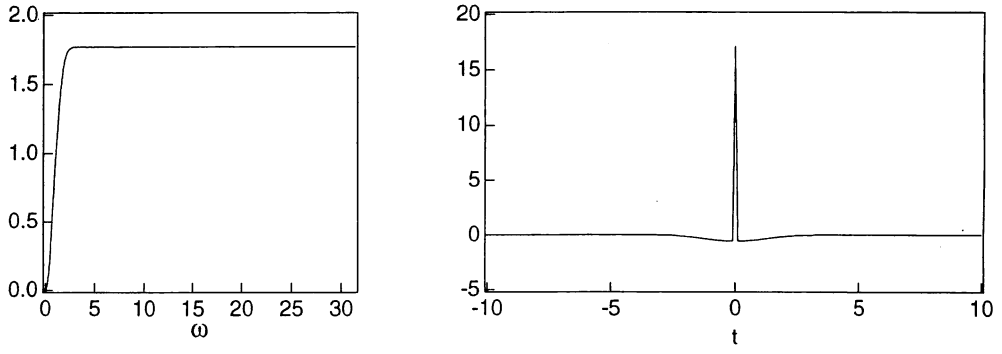

(c) Residual wavelet.

Figure 1 Analyzing wavelet, scaling function and residual wavelet for DOG wavelet transform ($M = 2$; Mexican hat). Left: Fourier spectra; right: waveforms.

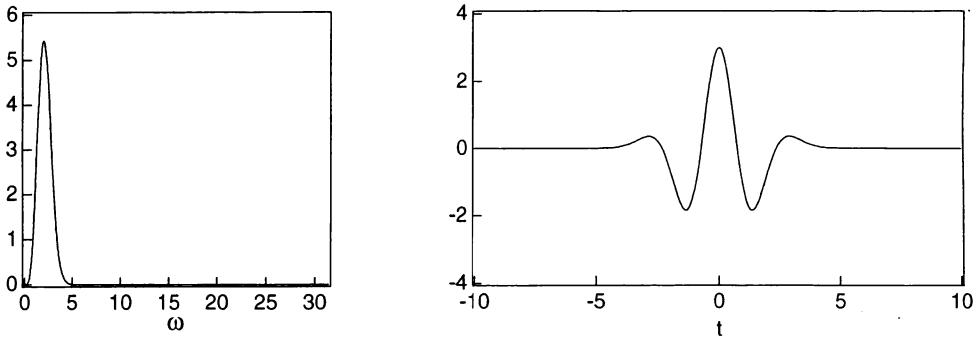

(a) Analyzing wavelet.

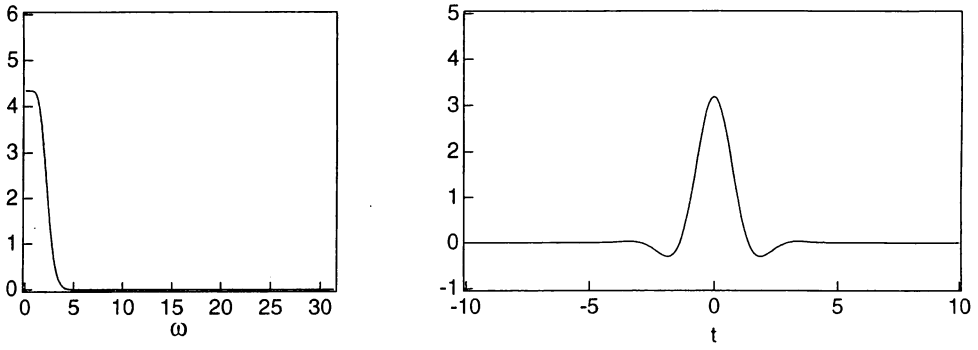

(b) Scaling function.

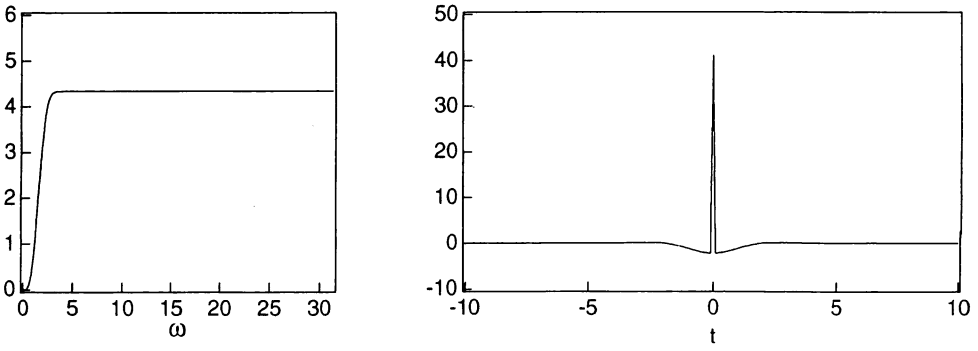

(c) Residual wavelet.

Figure 2 Analyzing wavelet, scaling function and residual wavelet for DOG wavelet transform ($M = 4$). Left: Fourier spectra; right: waveforms.

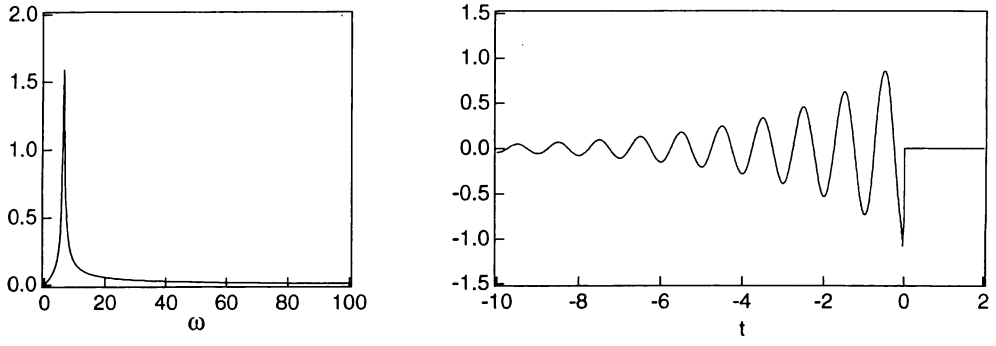

(a) Analyzing wavelet.

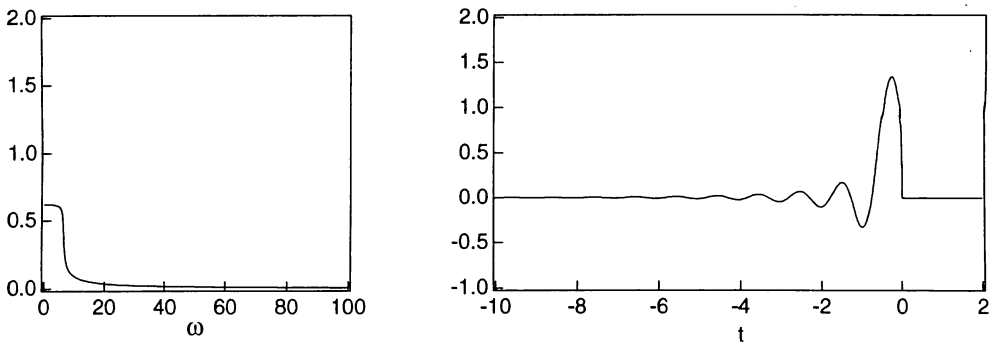

(b) Scaling function.

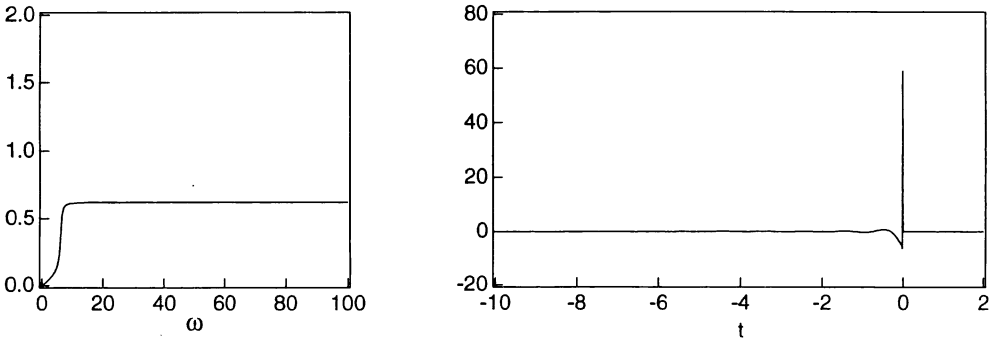

(c) Residual wavelet.

Figure 3 Analyzing wavelet, scaling function and residual wavelet for VR wavelet transform ($\zeta = 0.05$). Left: Fourier spectra; right: waveforms.

$$\sigma = \left(\frac{a_{\max}}{a_{\min}}\right)^{\frac{1}{J-1}},$$
$$b_k = k\Delta b,\ k = 0, 1, \cdots\cdots, N_j - 1, \tag{40}$$
$$\Delta b = a_j b_0,\ b_0 = \frac{1}{B}$$

where B is the bandwidth of the analyzing wavelet.

Another possibility is to use a homogeneous sampling grid for the shift parameter, i.e.,

$$b_k = k\Delta t,\ k = 0, 1, \cdots\cdots, N_j - 1 \tag{41}$$

where Δt is the sampling period of the data. However, this sampling manner could be very redundant in large scales and too coarse in small scales.

3.2 Aliasing of wavelets

Because we handle discrete data, aliasing could be a problem for wavelets at small scales. To avoid the aliasing, zeros are added in the frequency domain to expand the band-width of the data. This operation corresponds to an interpolation in the time domain.

3.3 FFT-based computation

In order to accelerate the computation of the convolution integrals in CWT and ICWT, calculating them in the frequency domain using the fast Fourier transform (FFT) is effective. The FFT-based computation is also suitable to the requirement for the band-width adjustment to avoid the aliasing errors.

4. Accuracy of Reconstruction

In order to evaluate the accuracy of the CWT/ICWT pair, a zero-mean white Gaussian signal is first transformed onto the time-scale plane by CWT, then reconstructed by ICWT. In this example, the duration of the signal is 30 s, and the sampling period is 0.01 s. We use the VR wavelets with $\zeta = 0.05$. The boundaries of scale parameter are taken as $a_{\min} = 0.05$ s and $a_{\max} = 2$ s.

The reconstruction error ratio, i.e., the ratio of the error norm to the signal norm, is evaluated with respect to the number of the scale grid. The results are shown in Fig. 4 With $J \geq 300$, we achieve the reconstruction error ratio less than 1%, that means the r.m.s. of the error is less than 1/100 of that of the original signal.

5. Conclusion

In this paper, several difficulties which may arise in computing CWT and ICWT were discussed, and some techniques to improve the accuracy of computation have been proposed. Using those techniques, we have achieved the reconstruction error ratio less than 1 % even for a random signal.

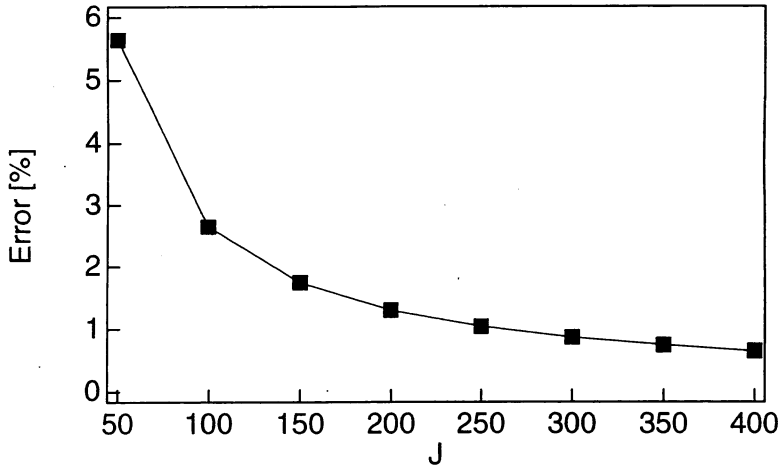

Figure 4 Reconstruction error ratio.

Department of Mechanical and System Engineering,
Faculty of Engineering and Design,
Kyoto Institute of Technology,
Matsugasaki, Sakyo-ku, Kyoto 606-8585, Japan

References

1) G. Kaiser, "A Friendly Guide to Wavelets", Birkhäuser, pp. 60-77 (1994).
2) O. Rioul and P. Duhamel, *IEEE Transaction on Information Theory,* 38, pp. 569-586 (1992).
3) A. Masuda and A. Sone, *Proceedings of the ASME PV & P Conf.,* PVP-Vol. 445-1, Seismic Engineering, pp. 175-180 (2002).
4) S. Mallat, "A Wavelet Tour of Signal Processing", second edition, pp. 67-219 (1999).
5) A. Masuda, M. Noori, A. Sone and Y. Hashimoto, *Proceedings of the 15th ASCE Engineering Mechanics Conference,* No. 208, pp. 1-8 (2002).
6) A. Papoulis, "Signal Processing", McGraw-Hill, pp. 227-231 (1977).